On the Use of Sweeping Langmuir Probes in Cutting Arc Plasmas—Part I: Experimental Results

Leandro Prevosto, Héctor Kelly, and Beatriz Mancinelli

***Abstract*—The first study of Langmuir probes applied to cutting arcs using a sweeping-probe system is presented. It is found that, under a relatively broad range of experimental conditions (changes in the probe material, in the probe radii, or in the sweeping frequency of the probes), no probe damage is registered, notwithstanding the large value of the power flux present with these arcs. In practice, probes with radii down to 63 μm and with sweeping rotation frequencies down to 8.7 s^{-1} (probe transit time of $\approx$140 μs through the arc) were used without noticeable alterations. In the measurements of the ion current collected by negatively biased probes, the following two unexpected features are found: the lack of a current plateau in the ion branch of the I–V probe characteristic and the independence of the signal amplitude on the probe radius. According to the experimental evidence, as well as several estimations, we have neglected electron emission of the probe surface as a relevant mechanism in modifying the ion branch of the characteristic. On the contrary, some arguments on which a collection model will be based are presented.**

***Index Terms*—Cutting arcs, Langmuir probes, plasma diagnostic.**

I. Introduction

PLASMA CUTTING is a process of metal cutting at atmospheric pressure by an arc-plasma jet, where a transferred arc is generated between a cathode and a work piece (the metal to be cut) acting as the anode. A high-quality cut requires a narrow, hot and high-velocity plasma jet, i.e., a high-energy-density arc jet. To this end, a new generation of cutting torches, the so called "high-energy-density torch" were developed. This new generation of torches is characterized by an arc-current intensity in the range of 30–100 A, flat cathodes, oxygen as the plasma gas, very small nozzle diameters ($\approx$1 mm), and the generation of an underexpanded supersonic arc jet with a shock wave close to the nozzle exit [1]–[4].

Due to the hostile conditions prevailing inside such atmospheric-pressure thermal plasmas, access to information about the plasma structure is usually gained through noninvasive spectroscopic techniques [1]–[3], [5]. While the interpretation of the experimental data is problematic, such techniques remain as the most useful and physically descriptive available in the high-pressure regime. However, Langmuir probes have also been used for plasma diagnostics in a wide range of experimental conditions [6]–[8]. Although invasive in nature, the technique is fast and relatively easy to apply, and it has been shown to be viable even at high pressure where the plasma temperatures considerably exceed the melting temperature of the probe [9]. To avoid probe damage, it is necessary to rapidly move the probe with respect to the plasma, which is usually employing sweeping probes. Unfortunately, the theory necessary for the interpretation of the probe current–voltage (I–V) characteristic in collision-dominated plasmas (in which the mean free paths of the charged particles are much smaller than the characteristic length of the probe) in terms of the plasma density and temperature is rather complicated [10]–[12].

While there is a large number of experimental works using Langmuir probes in the low-pressure regime, there is a very limited amount of published works concerning the investigation of high-pressure thermal plasmas (atmospheric and above) with such probes [6], [9], [13]–[15], and, to our knowledge, none in high-pressure high-velocity arc regimes (flow velocity of the order of the ion sound velocity) like cutting arcs.

Benilov and Rogov [16] presented a unified technique for the calculation of the ion-saturation current to cylindrical and spherical Langmuir probes in a uniform plasma, neglecting volume ionization and recombination in the sheath region. In Table 1 of Benilov's work, a collection of experimental data of several plasma experiments at atmospheric pressure was presented. That analytical technique describes most of these data within an accuracy of a factor three.

Gick *et al.* [15], on the basis of an observed flat ion-saturation-current curve, derived the radial temperature profile along the arc axis of an 8-mm-length 100-A 6–Nl/min^{-1} tungsten-inert-gas (TIG) welding arc. Using the classical low-pressure random ion-saturation-flux expression, a plasma temperature of about 10 kK was obtained at the arc axis at 4 mm from the cathode tip. The diameter of the molybdenum wires of the employed sweeping Langmuir multiprobe system was fixed to a value of 150 μm, and a saturation current of about 1 A was drained when the probe was biased by more than 20 V which is negative with respect to the anode. Recently, Fanara [13], [14], who was also using sweeping Langmuir probes (with a diameter of the copper wires fixed to a value of 250 μm) in TIG arcs, employed a version of the stationary low-pressure model of Gick *et al.* but modified to include streamline perturbations in the plasma flux due to the presence of the probe, thus producing orientation effects in its collecting surface (taken as two-thirds of the probe surface). Fanara considered also the noncollisionality of the sheath, i.e., the ion velocity at the sheath edge was chosen according to the Bohm criterion. Again, the employed

Manuscript received May 4, 2007; revised November 16, 2007. This work was supported in part by the University of Buenos Aires (Grant PID X111) and in part by CONICET (Grant PIP 2239/99).

L. Prevosto and B. Mancinelli are with the National Technological University, Regional Venado Tuerto, Venado Tuerto, 1347 Santa Fe, Argentina.

H. Kelly is with Institute of Plasma Physics, Consejo Nacional de Ciencias y Technología, Departamento de Física, Facultad de Ciencias Exactas y Naturales, Universidad de Buenos Aires, 1428 Buenos Aires, Argentina (e-mail: kelly@tinfip.lfp.uba.ar).

Digital Object Identifier 10.1109/TPS.2007.914176

technique to derive the plasma temperature was that based on the measurement of the ion-saturation current. For instance, a plasma temperature of about 11 kK was reported [14] on the axis in a 5-mm-length 100-A 10–Nl/min^{-1} TIG arc at 2 mm from the cathode tip. This temperature was compared with the spectroscopic measurements obtained with the Fowler–Milne technique, where an arc temperature of about 16.5 kK was measured on the arc axis at the same axial coordinate. In the author's conclusion, the discrepancies between both temperatures was due to the fact that the Langmuir probe technique in atmospheric-pressure arcs invariably yields depressed plasma temperatures.

More recently, Fang *et al.* [17] presented a computer simulation of the probe–flowing-plasma interaction. Attention was paid to the thermal and fluid dynamic disturbances caused by spherical probes situated on the arc axis of a typical TIG arc. Investigations were also carried out on the characteristic time required for the plasma and sweeping probes to reach a steady state. In particular, the influence of a spherical copper probe with a diameter of 250 μm on the arc axis at 2.5 mm of the cathode tip was investigated in a 200-A TIG arc. The surface temperature of the probe was fixed at the melting temperature of copper, and a nonslip condition was imposed for the velocity, but no conditions were imposed on the probe bias, i.e., the probe was in floating conditions. It was found under steady-state conditions that the presence of a solid, isolated, and cold probe severely affects the temperature and velocity fields of the arc. The effects of a sweeping probe through the plasma were also addressed. It was found that the time scale characterizing the temporal variations of the temperature and velocity was comparable with the traveling time of the probe across the arc diameter (approximately milliseconds). The author's conclusion was that the use of a Langmuir probe as a general diagnostic tool for thermal flowing plasmas was not yet a practical proposition.

Cutting arcs produce more hostile conditions than those found in TIG arcs. The cutting plasma velocities are around one order of magnitude higher than those reported for TIG's, and the cutting arc radius is correspondingly smaller and even comparable to the smallest probe size that can be considered to avoid probe damage. Hence, the power flux exceeds largely those that are found in thicker (welding) arcs. In this paper, we present the first study of Langmuir probes applied to cutting arcs using a sweeping-probe system as in the previous quoted works with TIG arcs. Special emphasis in this paper is given to the experimental procedure and to the experimental results where some unexpected results related to the probe characteristic and to the collecting probe area are found. In addition, the problem of probe heating is discussed with some detail. In an accompanying paper, a simplified theory is presented to interpret the experimental results and to infer plasma-quantity values from the probe measurements.

II. Experimental Arrangement

A. Arc Torch

The high-energy-density cutting torch used in this study consisted of a cathode centered above an orifice in a converging-straight copper nozzle. The cathode was made of copper (7 mm in diameter) with a hafnium tip (1.5 mm in diameter) inserted at the cathode center. A flow of oxygen gas cooled the cathode and the nozzle and was also employed as the plasma gas. The gas passed through a swirl ring to provide arc stability. The nozzle consisted in a converging straight bore (with a converging length of 1 mm and a bore that is 1 mm in diameter and 4.5 mm in length) in a copper holder surrounding the cathode (with a separation of 0.5 mm between the holder and the cathode surfaces). To avoid plasma contamination by metal vapors from the anode (usually the work piece to be cut), a rotating steel disk with a 200-mm diameter and 15-mm thickness was used as the anode [1]. Note that the arc considered is a transferred arc, and the anode disk is an essential part of the discharge and is not perturbing it. In this study, the disk's upper surface was located 5 mm from the nozzle exit. The arc was transferred to the edge of the disk, and the rotating frequency of the disk was equal to 185 s^{-1}. At this velocity, a well-stabilized arc column was obtained, and the lateral surface of the anode disc was not completely melted. Thus, practically, no metal vapors from the anode were present in the arc. A scheme of the torch indicating several geometric dimensions is shown in Fig. 1.

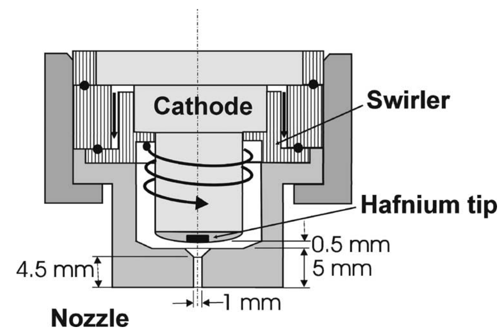

Fig. 1. Scheme of the arc torch indicating several geometric dimensions.

During arc operation, the voltage drop between the anode and the cathode (V_{CA}) and between the nozzle and the cathode (V_{NA}) were registered either by using a high-impedance (10 MΩ) voltage meter or by registering them on a digitizing oscilloscope. By performing a small orifice (1 mm in diameter) on the lateral of the cathode surface, the pressure in the plenum chamber (p_{ch}) was measured by connecting a pressure meter at the upper head of the cathode. The gas mass flow (dm/dt) injected in the torch was also registered. In this experiment, the arc current, the plenum pressure, and the gas mass flow were fixed to values of 30 A for the arc current, $p_{\mathrm{ch}} = 0.7$ MPa, and $dm/dt = 0.71$ g s^{-1}, respectively.

B. Multiprobe System

The multiprobe system which is employed for arc mapping is shown schematically in Fig. 2. It consists of a rotating aluminum disk carrying up to six identical probes that are mounted in the radial outward direction at different heights [9], [15]. The probes were made of tungsten or copper wires with radius R_p ranging from 63 to 250 μm, crimped on copper sleeves, and inserted in holes at different heights. This allowed the axial mapping of the arc in one single measurement with

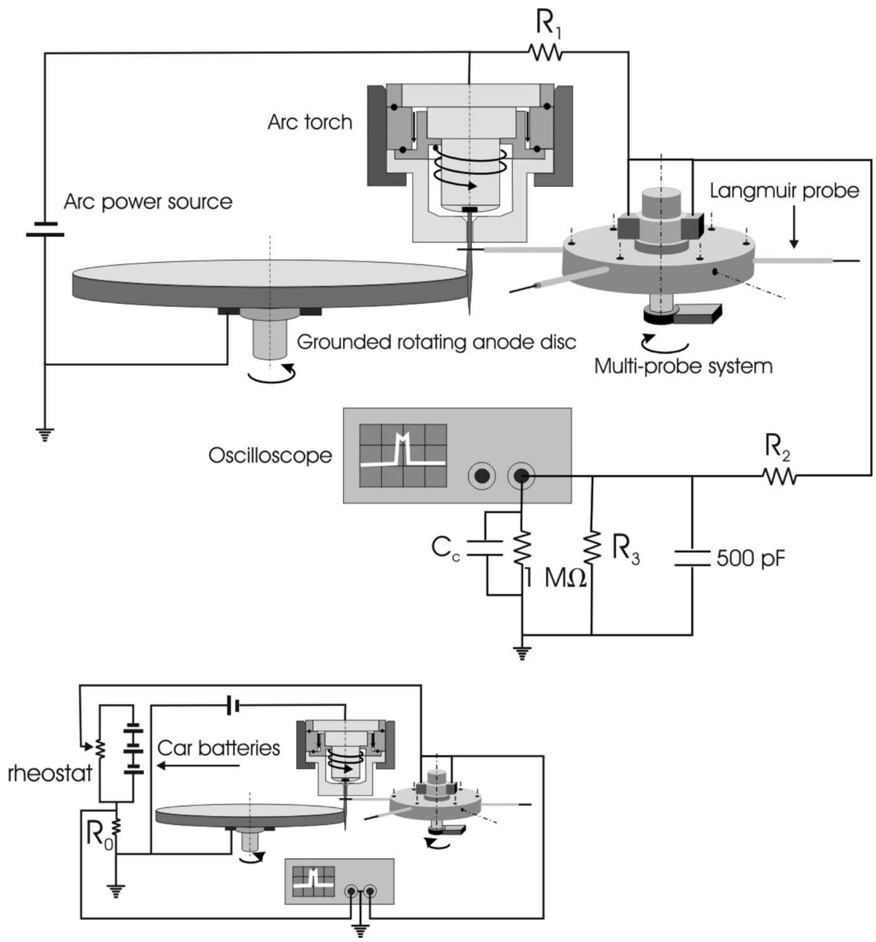

Fig. 2. Multiprobe system for mapping the arc. In addition, shown are the rotating anode, the arc electric circuit, and the two employed probe-biasing circuits. The bottom scheme represents the probe-biasing circuit with an independent power source.

a step of approximately 1 mm, starting at a height of 0.5 mm below the nozzle exit. The probes were swept through the arc at constant velocity in unbiased (floating) or negatively biased (probe potential below the plasma floating potential) conditions. The disc was rotated using a variable speed motor (with frequencies f in the range 8.7–43.7 Hz). On the upper disc surface, a pair of carbon brushes collected the probe current. The probes' length (55 mm) and the disc diameter (140 mm) were chosen to be large enough in order to consider that the probe axis was approximately parallel to the line joining the arc axis to the disc center during the whole passing of the probe through the arc and to ensure that the tip of the probe was well outside the arc column. Two different circuits were employed for biasing the probes; one of them used an independent biasing power source, whereas the other took advantage of the voltage distribution occurring in the main arc discharge and employed only resistors with appropriate values to bias the probe.

The two independent probe-biasing circuits are shown in Fig. 2. One of the biasing circuits used only a resistor (R_1, see Fig. 2) to bias the probe, whereas the second biasing circuit employed a set of three car batteries (12 V each) connected in series as an independent power source. To perform floating probe voltage measurements (with respect to the grounded anode and denoted by V_0), using the biasing circuit that does not use an independent power source, the resistance R_1 was disconnected, i.e., the probes were electrically isolated, and $R_2 = 10$ MΩ and $R_3 = 1$ MΩ. The capacity C_c in parallel with R_3 corresponded to that of the measuring coaxial cable (RG 58 U) and amounted to approximately 500 pF. Since the signals were registered with a digital oscilloscope with an input impedance of 1 MΩ (in parallel with 20 pF), the V_0 values were obtained in practice with a 21 times resistive voltage divider (as it will be shown in the next section, the duration of the V_0 signal of each probe was large enough as compared with the characteristic time of the 500-pF capacitor and the 0.5 MΩ equivalent resistance formed by the parallel between R_3 and the input resistance of the oscilloscope). The employed oscilloscope was a two-channel Tektronix TDS 1002 B with a sampling rate of 500 MS/s and an analogical bandwidth of 60 MHz. For the ion-current measurements, it was required to bias the probes below the plasma potential. Note from Fig. 2 that the resistance R_1 is in parallel with the resistance of the arc portion located between the probe position and the cathode; therefore, by adequately choosing the value of R_1, one can control the probe bias without using an independent biasing power source. In practice, R_1 was varied in the range of 40–340 Ω (thus varying the probe bias with a resistance value that is much larger than the arc resistance). The ion signal was registered in the oscilloscope by using a resistive voltage divider with an input impedance that is much larger than the R_1 value and with

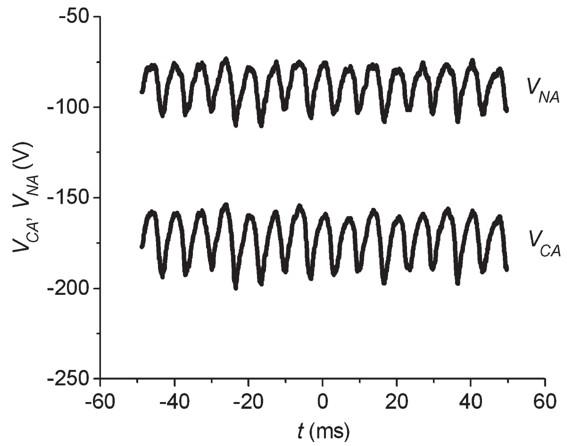

Fig. 3. Typical waveforms of the nozzle-anode (V_{NA}) and the cathode–anode (V_{CA}) voltages.

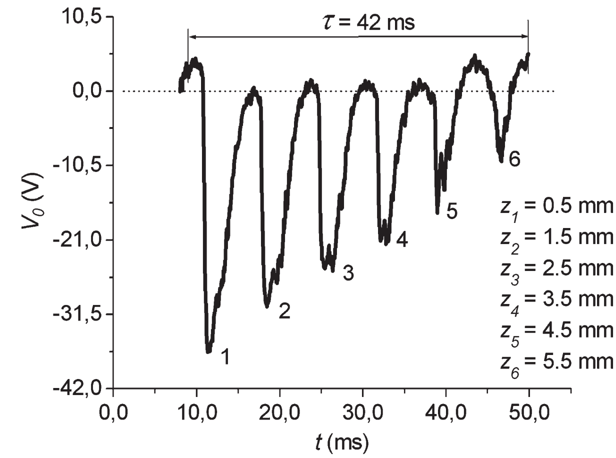

Fig. 4. Typical waveform showing the probe potential signals in floating conditions V_0 corresponding to six probes located at different axial coordinates (z) along the arc.

a measuring resistance (R_3) that is small enough so as to avoid distortions of the signal due to the discharge of C_c on R_3. In practice, the values $R_2 = 1$ KΩ and $R_3 = 12\ \Omega$ were found appropriate to accomplish the above quoted requirements, and the resulting signal attenuation was $\approx$1.18 10^{-2}.

As quoted before, a second biasing circuit using an independent power source was also employed to build the I–V probe characteristic. For the ion-current measurements, different probe bias voltages were obtained using a resistive voltage divider (rheostat) connected to the batteries. The probe current was calculated in this case from the voltage drop through a small resistance R_0 (see Fig. 2). The V_0 values were obtained simply by disconnecting the biasing circuit. Both methods of biasing the probes gave similar probe characteristic.

III. Experimental Results

Typical waveforms of V_{NA} and V_{CA} are shown in Fig. 3. It can be seen that both signals present an oscillatory component (with a frequency of 150 Hz) superimposed to a dc level that amounts to ≈ -85 V for V_{NA} and ≈ -175 V for V_{CA}. The oscillatory component was due to a ripple of the arc power source, and amounted to $\approx$10% of the corresponding dc value. The fluctuations of the dc value for different arc runs were relatively small (< 5%), and the dc values measured from the oscillographic waveforms were consistent with those obtained from the voltage meter.

We also checked that the arc voltage does not change during the probe sweeping through the arc.

A typical set of V_0 signals obtained with tungsten (W) probes with $R_p = 250\ \mu$m is shown in Fig. 4. The signal corresponds to six probes located at axial positions (z) in the range $z = 0.5$–5.5 mm, with a step of 1 mm ($z = 0$ corresponds to the nozzle exit). The sixth probe (that closest to the anode) was shorter (by 1.5 cm) than the other ones, which is in order to avoid touching the anode lateral surface. The time spacing between the individual peaks was in this case 7 ms, with a corresponding period of 42 ms for the whole set of probes. The rotating frequency of the probes was 23.8 Hz in this case (the probes velocity is $\approx$18 m/s with a radius of $\approx$12 cm at the arc position), which corresponds quite well with the previously quoted period. It can be seen on the time scale that each probe signal is very broad and, correspondingly, has a large thickness (several centimeters) on the spatial scale. Clearly, this thickness is not related to the actual arc radius (approximately millimeters), but can have contributions from a cold low-density plasma surrounding the arc core (generated by electron-heat conduction and radiation from the arc) and also from a probe capacitive coupling with the conductors configuration (anode, nozzle, and arc) that generate the potential distribution in all the volume surrounding the discharge (note that the sixth probe is not passing through the arc, but it is sensing a signal similar in shape to the other ones). Note also that these V_0 signals are further distorted by the ripple frequency of the arc power source, since the corresponding period (6.7 ms) is quite similar to the time between two consecutive probes transits through the arc. For the previously quoted reasons, we think that the shape of the V_0 signals does not give any information about the arc structure, and therefore, we have only taken (with certain confidence) the peak values of the signals as representative of the V_0 value at the arc position. For different arc runs, these peak values fluctuated somewhat around a mean value, with a statistical dispersion (over more than 20 arc runs) of about 3%. In Fig. 5, the average values of V_0 ($\langle V_0 \rangle$) are presented. Within the experimental uncertainties, it can be seen that $\langle V_0 \rangle$ increases almost linearly from the nozzle to the anode. Since, in high-pressure cutting arcs, the plasma temperature does not show marked variations with the axial coordinate along the arc region extending from the nozzle to the anode [1], [3], the axial electric field can be estimated from the axial profile of $\langle V_0 \rangle$. This procedure has also been used with TIG arcs [6], [9]. Thus, the behavior of $\langle V_0 \rangle$ indicates an almost constant axial electric field value ($\sim$7 V/mm) in the external part of the arc.

In Fig. 6, four typical probe-current waveforms of W probes with different R_p values (63, 100, 150, and 250 μm) for $z = 3.5$ mm, $R_1 = 140\ \Omega$, and $f = 23.8$ Hz are presented. The waveforms belong to different arc runs, but, for comparative purposes, they were plotted on a single time scale. Within experimental fluctuations, the traces are quite similar, showing an almost square shape with a duration of $\sim$50 μs (corresponding to an arc diameter of $\sim$0.8 mm) and with an ion-current

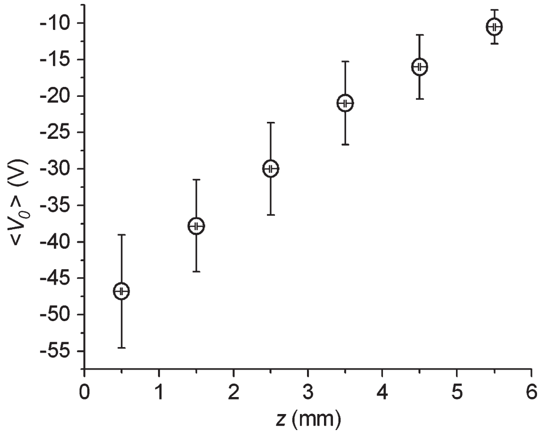

Fig. 5. Averaged probe potential in floating conditions $\langle V_0 \rangle$ as a function of the axial coordinate (z) along the arc.

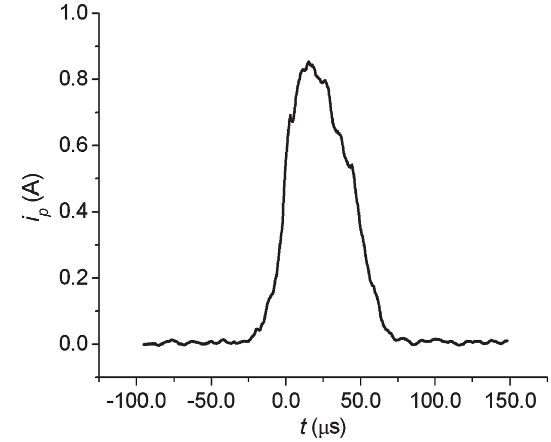

Fig. 7. Typical averaged (over 16 consecutive signals) ion-current probe signal.

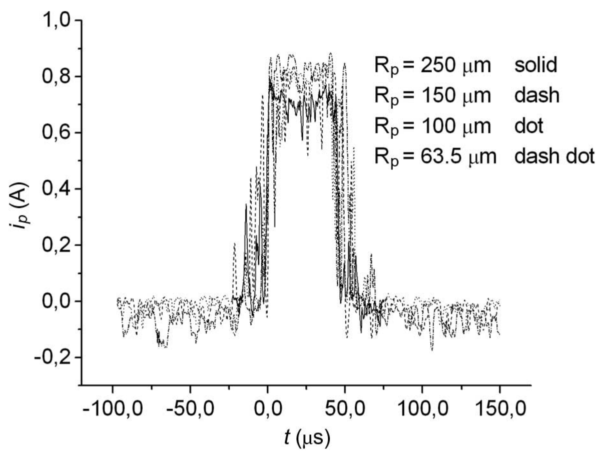

Fig. 6. Four typical current waveforms of W probes with different radii. $z = 3.5$ mm, $R_1 = 140\ \Omega$, and $f = 23.8$ Hz.

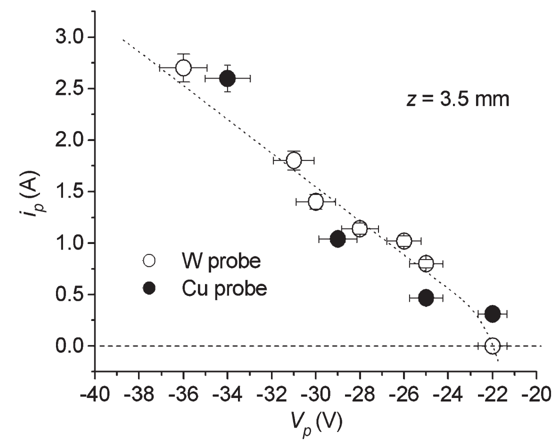

Fig. 8. Tungsten and copper probe I–V characteristics for $z = 3.5$ mm. The current values correspond to the peak values of the averaged signals.

amplitude of ~0.8 A. The square shape refers to a "smoothed" version of the signal that does not take into account the high-frequency noise appearing in the "top hat" profile of the measured signal. Note that this high-frequency noise is not associated to the arc-plasma structure, because it is also present on the base of the signal, when the probe is not in contact with the arc core.

Statistical fluctuations of these signals were not very large in current amplitude ($< 10\%$), but somewhat larger in the duration ($\sim 30\%$). The origin of such fluctuations can be explained in terms of the arc-voltage fluctuations (ripple) and the corresponding changes in the plasma-arc structure caused by this ripple. This explanation will be presented in the accompanying paper. The most impressive (and unexpected) result coming out from Fig. 6 is the independency of the ion-current amplitude on the probes size, notwithstanding the fact that the geometrical collecting area of the probes was changed by a factor of four.

In order to infer some meaningful information on the plasma properties from the probe signals, some smoothing of the fluctuations was performed by acquiring the signals using the 16 times average acquisition mode of the oscilloscope. In Fig. 7, it is shown as a typical averaged signal (W probe, $R_p = 250\ \mu$m, $z = 3.5$ mm, $f = 23.8$ Hz) that represents an average over 16 consecutive signals (this means that the average is performed over a time $\approx$1 ms). It can be seen that the amplitude of this signal remains at almost the same value of the individual peaks (small ion-current-amplitude fluctuations), but appears with a Gaussian-like shape due to the smoothing effect of averaging several individual square pulses with different duration.

Using the current peak value of the averaged signals, the current-voltage probe characteristic (mainly the ion branch) was built. This was done experimentally by varying the R_1 value (see Fig. 2), and the result for, $z = 3.5$ mm, is shown in Fig. 8, where the probe current i_{p} is plotted as a function of the probe potential V_{p} (measured with respect to the anode). Both tungsten- and copper-probe characteristics with $R_p = 250\ \mu$m have been included in Fig. 8 ($f = 23.8$ Hz). It can be seen that no current plateau (ion-saturation region) can be identified from Fig. 8, but the ion current grows approximately linear with (minus) the probe voltage, except in the vicinities of the V_0 value ($V_0 = -22$ V in this case). This result is in disagreement with published results [13]–[15] obtained with other types of atmospheric arc plasmas (TIG arcs). Since a possible explanation of the lack of an ion-saturation region could be given in terms of thermoionic electron emission from an overheated probe surface, we change the probe material, using Cu instead of the original W (see next section). However, it can be been from Fig. 8 that the I–V curves obtained with both materials are almost similar. In addition, we tried to identify an experimental condition where the probes were seriously damaged or even destroyed. However, changes in the probe material (W or Cu), in the probe radii (63–250 μm), or even in the rotating frequency of the probes holder (from 43.7 to 8.7 Hz) rendered negative results, which is in the sense that no damages in the probes could be detected.

IV. Discussion

One interesting point found in this work concerns the independency of the ion-probe current on the probe size. It should be mentioned that Tsuji and Hirano [18], working with very different plasma conditions (low flux velocity, low ionization degree), also found a very weak dependence of the ion current with the probe diameter. Clearly, there will be a collecting mechanism establishing that only a part of the probe surface, independent of the R_p value, is effective for ion collection. That part should be a small one, since a simple numerical calculation of the ion current based on ions arriving to the whole probe surface with thermal velocities would lead to ion currents much larger than those actually registered. Moreover, the effective ion-collecting-probe area should also be dependent on the local electric-field value in the probe vicinities to explain the lack of an ion-current saturation. Although a detailed explanation of these points will be presented in an accompanying paper (Part II), we will present here some general arguments on which a collection model is based because they will be useful to estimate the probe-surface heating.

A probe immersed in a high-pressure plasma is considered to be surrounded by a very thin noncollisional sheath (with a thickness of the order of the Debye length, $\approx 10^{-8}$ m in this case). The noncollisional sheath is followed (at increased radii) by a collisional presheath, with an electrically perturbed plasma density (according to the electric field value set by the probe bias) and with a thickness roughly of the order of the probe size. Beyond the presheath region, an "unperturbed" plasma region follows, in the sense that the electric field established by the probe bias does not penetrate this last region. However, it should be taken into account that, in this problem, the plasma has an hydrodynamic motion that can be represented far from the probe as an uniform flux with a fluid velocity close to the ion thermal velocity. The presence of the probe will induce a hydrodynamic modification of the otherwise straight flux streamlines that will affect both the plasma and the presheath regions at distances from the probe surface of the order of the probe radius. Close to the probe surface, the plasma flux will have high tangential velocities, mainly in the probe hemisphere facing the original uniform plasma flux. Fanara [13], [14], working with a TIG arc, took into account this hydrodynamic probe perturbation by assuming that the probe collected ions up to a point where the boundary layer separates from the probe surface and obtained two thirds of the probe area as the effective collecting surface. However, for cutting arcs where the flux velocities are around ten times larger than those reported with TIG arcs, there appears a limiting mechanism that is much more restrictive for defining the effective collection area than the boundary layer separation. This mechanism comes out from the fact that ions going into the probe surface move radially with a diffusive velocity acquired in the presheath region where a plasma-density gradient is established. Since these ions also have a tangential velocity whose value depends on the azimuth angle θ (measured with respect to an axial direction defined by the opposite to the uniform flux direction), the condition of arrival to the probe surface of an ion located at a given θ will depend on the ratio between its radial and tangential velocities at that angle. For instance, at the upper point of the probe surface (that facing the uniform flux with $\theta = 0$), all the ions will be collected because their tangential velocity is null at this point (stagnation point). Since, in cutting arc plasmas, the ion tangential velocities are very large, there will be a limited range of θ angles where the ions can reach the probe before they are dragged by the hydrodynamic flux eluding the probe surface. We will name θ_l as the limiting angle such that, for $0 < \theta < \theta_l$, all the ions are being collected by the probe.

Another point that is to be addressed in this work concerns the lack of an ion-saturation region in the I–V probe characteristic. The first candidate to explain this fact is the electron emission from the probe. This electron emission can be due to secondary emission processes (photon or ion-impact emission) or thermoionic emission. However, the temporal shape of the ion-probe current and the independency of this current with the probe radius (see Fig. 6) rules out photoelectron emission as a relevant mechanism because the spatial width of the ion signal roughly corresponds to the expected arc thickness, whereas the radiation field providing photons with enough energy to produce photoelectrons extends presumably over much larger radial distances. In addition, it is expected that eventual photoelectrons should be emitted from the whole probe surface. On the other hand, electron emission by ion-impact in an atmospheric-pressure torch operated with oxygen gas can be neglected since the effective secondary emission coefficient for oxygen ions is very small ($\sim 10^{-6}$, see [10]). The thermoionic emission from a highly heated probe surface deserves a more detailed analysis. On the one hand, Fig. 8 shows that the W- or Cu-probe characteristics are similar, in spite of the fact that, although both materials have similar work functions [10], their surface temperature can be very different. To go deep with this argument, we will present in what follows an estimation of the surface temperature of both materials.

From the diffusion heat equation, the thickness δ of the heated layer from the probe surface is given by

$$\delta \approx \sqrt{\frac{\kappa\tau}{\rho c}} \quad (1)$$

where κ, ρ, and c are the thermal conductivity, mass density, and specific heat of the probe material, respectively, and τ is the interaction time between the probe and the plasma (the transit time of the probe across the arc in this case). From (1), the probe mass heated by the plasma can be expressed as

$$M_p \approx \rho(2\theta_l R_p 2R_A)\delta \quad (2)$$

where the expression between the parenthesis in the right-hand side of (2) represents the effective collecting area of the probe (R_A is the arc radius).

The average temperature T_{a} (spatially averaged) of M_p can be obtained from a calorimetric equation for the probe, considering that the energy delivered to the probe surface by the plasma corresponds to that given by the ion energy flux. Taking into account that the delivered energy per ion is the sum of the kinetic ion energy plus the recombination energy, T_{a} can be expressed as

$$T_{\mathrm{a}} - T_0 \approx i_p \frac{|V_p - V_s| + \varphi_{\mathrm{i}}}{4\theta_l R_p R_A} \sqrt{\frac{\tau}{\rho c \kappa}} \tag{3}$$

where T_0 is the initial probe temperature (ambient), V_s is the unperturbed plasma potential, and φ_{i} is the ionization potential of the gas (atomic oxygen in this case). Alternatively, an estimation of the probe-surface temperature (T_{s}) can be obtained by seeking for the classical solution of the 1-D thermal diffusion equation with a given energy flux at one extremum ($x = 0$) and $T \rightarrow T_0$ at large x values. In this case, it is obtained as

$$T_{\mathrm{s}} - T_0 \approx 2 \left[i_p \frac{|V_p - V_s| + \varphi_{\mathrm{i}}}{4\theta_l R_p R_A} \right] \sqrt{\frac{\tau}{\rho c \kappa}}. \tag{4}$$

As it can be seen, (3) and (4) differ only by a factor of two in both estimated temperatures. For instance, we can estimate T_{s} from (4) for our experimental conditions. Taking $i_p = 2.7$ A (the largest ion current experimentally registered), $|V_p - V_s| \approx 24$ V, $\theta_l \approx 10^\circ$ (see accompanying paper), $R_p = 250$ μm, $\varphi_{\mathrm{i}} = 13.6$ eV, $\tau = 50$ μs, $R_A = 0.5$ mm, and $T_0 = 300$ K, it is obtained as follows:

1) $T_{\mathrm{s}} \approx 1000$ K($\rho = 1.93\,10^4$ kg m^{-3}, $\kappa = 174$ W m^{-1} K^{-1}, $c = 132$ J kg^{-1} K^{-1} [18]) for W.
2) $T_{\mathrm{s}} \approx 700$ K ($\rho = 0.9\,10^4$ kg m^{-3}, $\kappa = 401$ W m^{-1} K^{-1}, $c = 385$ J kg^{-1} K^{-1} [18]) for Cu.

It can be seen that both T_{s} values are well below the melting temperatures of both metals, which is in agreement with the experimental results that showed no probe damage. In addition, at these relatively low temperatures, the thermoionic current density from the probe's surface is given by the Dushman–Richardson formula, which is corrected by the Schottky effect [10] (the extracting electric field developed within the sheath with and extension of few λ_D can reach $\approx 10^8$ Vm^{-1}). Even considering an eventual reduction in the work function from the 4.54 eV of W and 4.4 eV of Cu to about 2 eV (due to metal oxidation in an oxygen plasma), the thermoionic current density from the probes are $\approx 10^3$ Am^{-2} for the W case and ≈ 1 Am^{-2} for Cu, which are completely negligible compared with the actual ion-current density at the probe surface $\approx 10^7$ Am^{-2}. This is in agreement with the experimental results that showed a similar behavior in the I–V curves obtained with both materials

V. Final Remarks

We have presented in this work the first sweeping Langmuir probe measurements in a cutting arc. It was found that, under a relatively broad range of experimental conditions (changes in the probe material, in the probe radii, or in the sweeping frequency of the probes), no probe damage was registered, notwithstanding the large value of the power flux present with these arcs. In practice, probes with radii down to 63 μm and with sweeping rotation frequencies down to 8.7 s^{-1} (probe transit time of ≈ 140 μs through the arc) were used without noticeable alterations.

The information on the arc structure that can be obtained from a probe in floating conditions is very limited, since the signal registered by the probe includes not only the arc itself but also a broad region (several cm thick) extending radially outside the arc that reflects the presence of a weakly ionized plasma surrounding the arc core.

In the measurements of the ion current collected by negatively biased probe, the following two unexpected features were found: the lack of a current plateau in the ion branch of the I–V characteristic and the independence of the signal amplitude on the probe radius. According to the experimental evidence, as well as several estimations, we have neglected electron emission of the probe surface as a relevant mechanism in modifying the ion branch of the characteristic. On the contrary, we have presented some arguments on which a collection model (able to explain the ion-branch features of the probe characteristic) will be based. A detailed description of this model is the subject of an accompanying paper.

References

[1] P. Freton, J. J. Gonzalez, A. Gleizes, F. C. Peyret, G. Caillibotte, and M. Delzenne, "Numerical and experimental study of a plasma cutting torch," *J. Phys. D, Appl. Phys.*, vol. 35, no. 2, pp. 115–131, 2002.

[2] P. Freton, J. J. Gonzalez, F. C. Peyret, and A. Gleizes, "Complementary experimental and theoretical approaches to the determination of the plasma characteristics in a cutting plasma torch," *J. Phys. D, Appl. Phys.*, vol. 36, no. 11, pp. 1269–1283, 2003.

[3] L. Girard, P. Teulet, M. Razafinimanana, A. Gleizes, F. C. Peyret, E. Baillot, and F. Richard, "Experimental study of an oxygen cutting plasma torch: I. Spectroscopic analysis of the plasma jet," *J. Phys. D, Appl. Phys.*, vol. 39, no. 8, pp. 1543–1556, Apr. 2006.

[4] P. Teulet, L. Girard, M. Razafinimanana, A. Gleizes, P. Bertrand, F. C. Peyret, E. Baillot, and F. Richard, "Experimental study of an oxygen cutting plasma torch: II. Arc-material interaction, energy transfer and anode attachment," *J. Phys. D, Appl. Phys.*, vol. 39, no. 8, pp. 1557–1573, Apr. 2006.

[5] C. Pardo, J. González-Aguilar, A. Rodríguez-Yunta, and M. A. G. Calderón, "Spectroscopic analysis of an air plasma cutting torch," *J. Phys. D, Appl. Phys.*, vol. 32, no. 17, pp. 2181–2189, 1999.

[6] C. J. Allum, "Power dissipation in the column of a TIG welding arc," *J. Phys. D, Appl. Phys.*, vol. 16, no. 11, pp. 2149–2165, Nov. 1983.

[7] D. W. George and P. H. Richards, "Boundary conditions in wall-stabilized arc columns," *J. Phys. D, Appl. Phys.*, vol. 1, no. 9, pp. 1171–1182, Sep. 1968. ser. 2.

[8] C. S. MacLatchy and H. C. L. Smith, "The electron current to a Langmuir probe in a flowing high-pressure plasma," *IEEE Trans. Plasma Sci.*, vol. 19, no. 6, pp. 1254–1258, Dec. 1991.

[9] C. Fanara and I. M. Richardson, "A Langmuir multi-probe system for the characterization of atmospheric pressure arc plasmas," *J. Phys. D, Appl. Phys.*, vol. 34, no. 18, pp. 2715–2725, Sep. 2001.

[10] Y. P. Raizer, *Gas Discharge Physics*. Berlin, Germany: Springer-Verlag, 1991.

[11] M. S. Benilov, "Can the temperature of electrons in a high-pressure plasma be determined by means of an electrostatic probe?" *J. Phys. D, Appl. Phys.*, vol. 33, no. 14, pp. 1683–1696, Jul. 2000.

[12] H. Schmitz and K. U. Riemann, "Consistent analysis of the boundary layer of a Saha plasma," *J. Phys. D, Appl. Phys.*, vol. 34, no. 8, pp. 1193–1202, Apr. 2001.

[13] C. Fanara, "Sweeping electrostatic probes in atmospheric pressure arc plasmas—Part I: General observations and characteristic curves," *IEEE Trans. Plasma Sci.*, vol. 33, no. 3, pp. 1072–1081, Jun. 2005.

[14] C. Fanara, "Sweeping electrostatic probes in atmospheric pressure arc plasmas—Part II: Temperature determination," *IEEE Trans. Plasma Sci.*, vol. 33, no. 3, pp. 1082–1092, Jun. 2005.

[15] A. E. F. Gick, M. B. C. Quigley, and P. H. Richards, "The use of electrostatic probes to measure the temperature profile of welding arcs," *J. Phys. D, Appl. Phys.*, vol. 6, no. 16, pp. 1941–1949, Oct. 1973.
[16] M. S. Benilov and B. V. Rogov, "Ion saturation current to spherical electrostatic probes in collisional plasmas," *J. Appl. Phys.*, vol. 70, no. 11, pp. 6726–6731, 1991.
[17] M. T. C. Fang, J. L. Zhang, and J. D. Yan, "On the use of Langmuir probes for the diagnosis of atmospheric thermal plasmas," *IEEE Trans. Plasma Sci.*, vol. 33, no. 4, pp. 1431–1442, Aug. 2005.
[18] H. Tsuji and T. Hirano, "Ion-current distributions around an electrically conductive body in ionized gas flow," *AIAA J.*, vol. 11, no. 1, pp. 100–102, 1972.
[19] H. L. Anderson, *A Physicist's Desk Reference*, 2nd ed. New York: AIP, 1989.

Leandro Prevosto was born in Santa Fe, Argentina, on November 29, 1971. He received the degree in electromechanical engineering from the National Technological University, Venado Tuerto, Santa Fe, Argentina, in 2005.

Since 2006, he has been on a fellowship with the Fundación Yacimientos Petrolíferos Fiscales, Argentina, and has been conducting Ph.D. studies with the Institute of Plasma Physics, Consejo Nacional de Ciencias y Tecnología, Departamento de Física, Facultad de Ciencias Exactas y Naturales, Buenos Aires, Argentina, and the Engineering University of Buenos Aires.

Héctor Kelly was born in Mendoza, Argentina, on February 14, 1948. He received the M.S. and Ph.D. degrees in physics from Buenos Aires University, Buenos Aires, Argentina, in 1972 and 1979, respectively.

Since 1973, he has been a researcher with the Plasma Physics Laboratory, Faculty of Sciences, University of Buenos Aires, and the Institute of Plasma Physics, Consejo Nacional de Ciencias y Tecnología (CONICET), Departamento de Física, Facultad de Ciencias Exactas y Naturales, Buenos Aires. His current research interests are high-power electric discharges, vacuum arcs, and nonthermal high-pressure plasmas. Since 1980, he has been a researcher with CONICET.

Beatriz Mancinelli was born in Santa Fe, Argentina, on February 6, 1965. She received the degree in Nuclear Engineering from the Balseiro Institute, San Carlos de Bariloche, Argentina, in 1990. She is currently working toward the Ph.D. degree in the Institute of Plasma Physics, Consejo Nacional de Investigaciones Científicas y Técnicas (CONICET), Departamento de Física, Facultad de Ciencias Exactas y Naturales, Universidad de Buenos Aires, Buenos Aires, Argentina, under a fellowship from the National Technological University, Córdoba, Argentina.